J Mater Sci: Mater Electron (2022) 33:3786–3800

Evaluation of superconducting features and gap coefficients for electron–phonon couplings properties of MgB_2 with multi-walled carbon nanotube addition

N. Kaya[1], S. Cavdar[2], O. Ozturk[3], G. Yildirim[4,*], and H. Koralay[2]

[1] Opticianry Program, Vocational School, T.C. İstanbul Arel University, 34290 İstanbul, Turkey
[2] Superconductivity and Thermal Analysis Laboratory (STAL), Department of Physics, Gazi University, 06531 Ankara, Turkey
[3] Department of Electrical and Electronics Engineering, Kastamonu University, 37100 Kastamonu, Turkey
[4] Department of Mechanical Engineering, Bolu Abant İzzet Baysal University, 14100 Bolu, Turkey

Received: 19 July 2021
Accepted: 10 December 2021
Published online: 23 January 2022

ABSTRACT

In this study, the samples are prepared by solid state reaction method at different weight ratios (0–4%). The characterization of materials produced is conducted with the aid of powder X-ray diffraction (XRD), temperature-dependent electrical resistivities (ρ-T) and magnetization (M–H) measurements. Moreover, the change in the scattering/breaking of cooper-pairs in the small homogeneous clusters in the superconducting paths with the addition of multi-walled carbon nanotube is also examined by the energy gap coefficients. All the experimental findings show that the weight ratio of wt 2% is observed to be the optimum addition level. The XRD results indicate that the MgB_2 material prepared by the optimum level crystallizes better in hexagonal symmetry. The critical current density is found to increase from 1.0×10^4 to 2.3×10^4A cm^{-2} depending on the increment in the magnetization values. On the other hand, the addition mechanism is noted to degrade slightly the general electrical features, critical transition temperatures, lattice cell constants and crystallite size of MgB_2 material. Regardless, although the carbon nanotube addition seems to be negative effect on some general properties, the fundamental characteristic properties (the crystallinity with smoother crystallographic transition, magnetization values, coupling of adjacent layers, degree of broadening and especially formation of effective nucleation centers for the flux pinning ability) improve seriously at the optimum dopant level. Thus, the MgB_2 prepared with the optimum carbon nanotube concentration can exhibit higher performance against the magnetic field and current in larger magnetic field strengths applied.

Address correspondence to E-mail: yildirim_g@ibu.edu.tr

https://doi.org/10.1007/s10854-021-07570-2

1 Introduction

With the discovery of the superconductivity in the binary MgB_2 compound in the year of 2001 by Akimitsu et al. [1], the scientists have shifted their fundamental focus to the materials due to their upper critical field (∼ 40 T) and higher critical temperature (∼ 39 K). Similarly, unique combinations of superior features including easy availability, lightweight, low anisotropy, low-cost of starting chemicals, simple crystal structure, strong intergranular bonds, fast/simple preparation procedure, long coherence length, possibility to work with cryocoolers around 20 K, fabrication of materials in multifilamentary wire, cable, sheets and plates (because of no weak-link behavior at grain boundaries) allow MgB_2 material to use in the heavy-industrial technology and energy-related sectors. On the other hand, low irreversibility field and flux pinning capacity as classic problems of MgB_2 material need to be improved by the proper production procedures such as dopant and material composition quantity/type, heat-treatment methodology, calcination/annealing ambient conditions (temperature, time and gas atmosphere), palletizing procedure (applied force and duration) and producing mechanism (chemical substitution, addition, doping, evaporation of transition metal on the surface, multi-layered and metallic interfaced structures) [2]. In this respect, the concept and improvement efforts of physical properties for the MgB_2 compound have recently attracted a lot of interest of several research communities [3, 4]. In some studies, many different materials as regards Co [5], Fe_3O_4 [6], Al [7], Na_2CO_3 [8] have been added in the crystal structure of MgB_2 so that the compound can find more places in the engineering application fields in the temperature range of 20–30 K. Although there appears both positive and negative effects of dopant mechanism in the MgB_2 crystal system, the carbon atoms or carbon related additives exhibit relatively more positive effects on the MgB_2 material as compared to the other additives. This is because, the carbon with high chemical reactivity (leading to the large specific surface area [9]) is known to be one of the most effective doping materials to improve remarkably the critical current density at higher external magnetic fields by modifying the B planes in the MgB_2 crystal structure [10]. Likewise, of several scientific studies reported in the literature the carbon atom or carbon related additives (SiC, hydrocarbons, carbon nanotubes) are found to be effective for the increase in the flux pinning ability, irreversibility field and upper critical field as a result of the substitution of B for C in the MgB_2 crystal lattice [9, 11, 12]. Moreover, it is observed that the addition of carbon nanotubes in the superconducting system makes the Mg and B powders easily agglomerate during the solid–solid mixing as a consequence of inherit large surface energy of powders [13]. Following the discovery, many researchers have experimentally tried to add the different amounts of carbon with the aid of various production methods in the main crystal matrix of MgB_2 [14–17].

It is well known that the carbon nanotubes discovered by Sumio Iijima in 1991 [18] present the good physical properties such as thermal, structural, mechanical, and mainly electrical conductivity [19]. There are a number of studies [20–27] in the literature where the researchers have examined the fundamental role of carbon nanotubes on the physical properties of MgB_2 material. It is noted that the carbon nanotube addition shows many advantages for the MgB_2 in comparison with the other addition materials [28]. To illustrate, the carbon nanotube addition is found to improve especially the critical current density of bulk MgB_2 material [21].

In the current study, the influence of multi-walled carbon nanotube (with the valuable positive physical properties) within the different weight ratios in the MgB_2 crystal structure on the phase purity, crystallinity quality, lattice cell constants, crystallite size, texturing, magnetization values, critical current densities, formation/destruction of flux pinning centers, coupling/decoupling of adjacent layers and beginning point of magnetic field penetration is examined. We also determine the variation of energy gap coefficients for the σ gap and π gaps, scattering/breaking mechanism of super-electrons, offset/onset critical transition temperatures, degree of broadening and fundamental electrical quantities including the normal state resistivity at room temperature (ρ_{300K}), residual resistivity (ρ_{res}), residual resistivity ratio (RRR), active cross-sectional area fraction (A_F), ρ_{40K}, ρ_{norm}, and $\Delta\rho$ parameters. The experimental findings display that the optimum multi-walled carbon nanotube level (wt. 2%) is a wise choice for the permanent and radical solutions for the global energy requirements.

Shortly, the remaining parts of paper are as follows:

- In Results and discussion part, the changes of fundamental characteristic behaviors including the crystal structure quality, electrical, superconducting, magnetization, coupling of adjacent layers, flux pinning capability, energy gap coefficients for the σ gap and π gaps are studied,
- In Sect. 3.1, experimental measurement results of XRD analyses are determined,
- In Part 3.2, hysteresis curves of pure and multi-walled carbon nanotube added MgB_2 superconductors are investigated,
- In Sect. 3.3, critical current density calculations based on Bean Model are performed,
- In Part 3.4, electrical findings founded on dc resistivity measurements are explored,
- In Sect. 3.5, Change of superconducting characteristic properties of MgB_2 with multi-walled carbon nanotube addition is analyzed,
- In Sect. 3.6, Variation in gap coefficients for electron–phonon couplings of carbon nanotube added MgB_2 materials is discussed,
- In Part 4, a brief review of main results is provided.

2 Methods

2.1 Experimental parts

In this study, magnesium (Mg) powder (> 99% purity, Sigma Aldrich), amorphous nano boron (B) powder (≥ 95% purity, Sigma Aldrich) and multi-walled carbon nanotube powders (≥ 90% purity, Sigma Aldrich) are used to produce new systems of MgB_2 + C. Firstly, according to the nominal composition in the crystal system 5 g of magnesium and amorphous nano boron powders are mixed with Retsch PM 400 automatic mixer for 3 h to obtain the homogenous powder of chemicals. The resultant powders are separately weighed to be 1 g for the five samples. Then, the multi-walled carbon nanotubes within the different weight ratios (wt 0–4%) are added in the MgB_2 + C samples. After then the powders are separately grounded by the grinder for half an hour in the agate mortar. The powder of mixture is named with five different codes. Namely, the reference sample will hereafter be shown as 0 or pure whereas the superconducting materials added with the different multi-walled carbon nanotube ratios of 1, 2, 3 and 4% will be called as 1, 2, 3 and 4 sample, respectively.

Every powder of mixture is pressed under 200 MPa pressure with a Specac brand hydraulic pressing tool to prepare in the bulks with a diameter of 13 mm. The cylindric bulks wrapped in the tantalum foils are heated up to 650 °C with a heating rate of 5 °C min^{-1} and annealed in an argon atmosphere for 1 h. X-ray diffraction analyses of cylindric samples obtained are performed by Rigaku Mini Flex 2 Brand X-ray diffractometer. The change in the fundamental crystalline properties of carbon nanotube added bulk MgB_2 superconducting compounds is examined with a 1.5418 Å wavelength source at the room temperature. The experimental data are gathered using 40 kV acceleration voltage in 2θ = 20°–80° at a scan speed of 2° min^{-1} with 0.02° step increment. Indexation of diffraction peaks is performed according to JCPDS index cards. One can see the experimental XRD diffraction patterns with Miller indices in Fig. 1 where all the materials produced exhibit the polycrystalline superconducting phase. At the same time, the crystal size of samples is calculated by Scherrer Equation [29] as provided in Eq. 1

$$D = \frac{K\lambda}{\beta \cos\theta}, \tag{1}$$

here the abbreviation of D is defined as the crystallite size (in the unit of nm), K defines Scherrer constant (0.9) and λ presents the wavelength (0.15418 nm) of beam emitted from the X-ray source. β also displays the full width at half maximum (FWHM) in radians of strongest peak when θ shows Bragg angle. Likewise, we determine the role of multi-walled carbon nanotube on the lattice strain and dislocation density in the MgB_2 crystal system using the following equations, respectively:

$$\varepsilon = \beta \cos\frac{\theta}{4}, \tag{2}$$

$$\delta = 15\frac{\varepsilon}{ad}, \tag{3}$$

where the abbreviation of ε is directly related to the lattice strain when a and d constants are associated with the lattice cell and grain size parameter, respectively.

Besides, the critical transition temperature values are measured by means of a LCR Meter ST2826 device when the magnetization measurements are

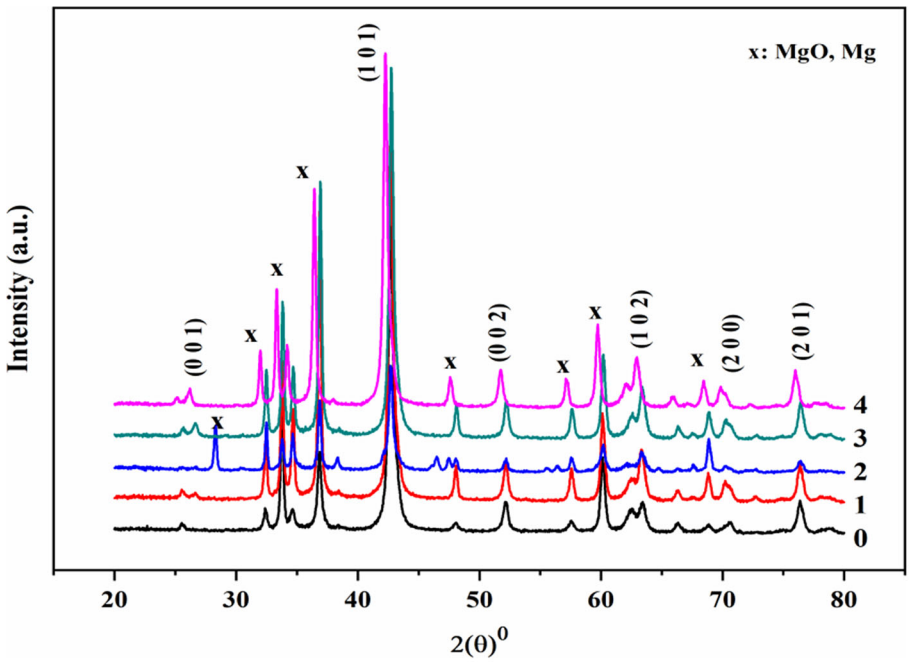

Fig. 1 X-ray diffraction patterns for all compounds

carried out with Lake Shore VSM device. The critical current density calculations are conducted by Bean method [30], the mathematical formula of which is shown in Eq. 4.

$$I_c = 20\frac{\Delta M}{a\left(1-\frac{a}{sb}\right)} \tag{4}$$

In the equation the constants of a and b are the width and thickness of material studied, respectively. Besides, the abbreviation of $\Delta M = (M_+ - M_-)/V$ ascribes to the electromagnetism of unit volume. Further, the magnetization values of $M_+ - M_-$ parameters are related to the zero-field values of different loops at various maximum fields.

3 Results and discussion

3.1 Experimental measurement results of XRD analyses

According to Fig. 1, there is a consistent change in the diffraction peak intensity and positions. Small differentiations stem from the off-stoichiometry of lattice due to the formation of new bonding between the atoms, different chemical valence (different electron configurations of outer shell), easier or harder integration with the surrounding atoms, difference in ionic radii of addition and host atoms. This is attributed to the fact that the multi-walled carbon nanotubes are successfully incorporated into the MgB_2 crystal system. However, it is to be mentioned here that the variations in the peak positions or intensities with the addition mechanism are not enough to claim any new phase formation in the crystal matrix.

It is also obvious from the figure that all the materials prepared in the current work present predominantly the main characteristic plane peaks due to the diffracted beams of MgB_2 superconducting system although there are a few other impurity phases such as MgO and Mg peaks (indicated by the notations of "*x*") due to the decomposition of the MgB_2 phase. Namely, the MgB_2 material can thermodynamically be decomposed into different phases such as MgB_4, MgB_6, MgB_{12} and MgO at higher temperatures due to the unstable characteristics of MgB_2 phase. Thus, with the increase in the carbon nanotube addition (impurity) in the MgB_2 superconducting materials, the decomposition of MgB_2 and oxidation of Mg are totally normal at elevated temperatures [31]. Regardless, the appearance of impurity phases in the minimal level in the MgB_2 superconducting matrix is not strong enough to affect seriously the main crystal system. It is another striking point deduced from this work that the peak intensity reflected along (101) diffraction plane is found to be the highest intensity among those of other plane reflections.

In more detail, of the compounds studied the diffraction peak (101) width of sample 2 is observed to be much narrower and more severe as compared to that of other samples. It is well known that the increment in the narrow of widths and intensity of peaks for the diffracted beams in X-ray diffraction patterns points out smoother crystallographic transition (favored by "*Change of superconducting characteristic properties of MgB_2 with multi-walled carbon nanotube addition*" part). This means that the material better crystallizes in the hexagonal symmetry [32]. On this basis, it is not wrong to confirm that the sample 2 presents much more uniform crystallographic structure than the other ones.

Furthermore, it is obtained that the widths of partial diffraction peaks enlarge with the presence of multi-walled carbon nanotube in the MgB_2 crystal lattice. In fact, the increase in the addition level leads to much more enhances the peak widths. The similar results can be encountered for the effect of graphite structures on the compounds in the literature [33]. Accordingly, the diffraction peaks appeared enable us to determine the effect of multi-walled carbon nanotube addition on the crystallite size of MgB_2 crystal system using the Scherrer–Warren approach provided in Eq. 2. In this regard, we find the full width at half maximum (FWHM associated with crystallinity and lattice defects [34]) for the predominant and strongest peak of (101) diffraction plane. The FWHM values are found to be about 0.370°, 0.404°, 0.397°, 0.401° and 0.372° for the pure, 1, 2, 3 and 4 samples, respectively. The change in the FWHM values leads to sensitively vary the lattice strain, crystallite size, phase composition and lattice cell parameters. In this respect, the crystallite sizes are found to be about 21.503 nm, 21.369 nm, 20.027 nm, 19.832 nm and 19.684 nm for the pure, 1, 2, 3 and 4 samples, respectively. Based on the experimental findings, the change in the crystallite size values results from the differentiation in the permeant lattice strains of MgB_2 crystal system. On this basis, it is easily anticipated that the pure sample presents the minimum lattice strain value of 6.90×10^{-2} whereas the sample 4 possesses the maximum strain value of 7.30×10^{-2} in the crystal structure (Table 1).

Besides, we determine the relative dislocation density ratios with respect to the pure sample and tabulate numerically in Table 1. It is apparent from the table that the highest value for the relative dislocation density ratio is calculated to be about 24.159 for the sample 4.

At the same time, the effect of multi-walled carbon nanotube addition on the relative phase volume fractions is determined using Eq. 5 to confirm the results observed in the XRD measurements. The phase percentage values belonging to the materials produced can be seen in Table 1. It is visible from the table that the characteristic MgB_2 superconducting phase tends to decrease systematically with the increment in the addition level. In this respect, the pure sample exhibits the phase volume fractions of 72% and 28% for the MgB_2 phase and impurity phases (related to the Mg and MgO phases), respectively. As for the sample 4, the phase percentage of MgB_2 superconducting phase decreases towards 61% when the impurity phase fraction increases up to 39%. The variation of phase percentages with the addition level clearly affects the lattice strain, crystallite size and lattice cell parameters of MgB_2 crystal system.

$$f_{MgB_2} = \frac{\sum I_{MgB_2(hkl)}}{\sum I_{MgB_2(hkl)} + \sum I_{Mg+MgO(hkl)}} \tag{5}$$

As for the computation of lattice cell parameters confirming the shift of partial diffraction peaks, we calculate the a and c parameters for the hexagonal unit cell structure using the equation of $1/d_{hkl}^2 = 4/3\left[h^{2+hk+k^2}/a^2\right] + l^2/c^2$ with the aid of the least square method through lattice spacing d values (related to the path difference between two waves undergoing interference) and (hkl) diffraction planes. The a and c lattice parameters of all the superconducting materials are numerically listed in Table 1. It is obvious from the table that the pure sample possesses the maximum a and c-axis lengths of 3.081 Å and 3.519 Å whereas the minimum cell parameters of 3.069 Å and 3.476 Å ascribe to the sample 4. All in all, the sample 2 shows the best crystallinity with the improved interaction between the coupling superconducting grains in the adjacent layers whereas the pure sample obtains the largest grain size and lattice cell parameters. The similar results can be encountered in the scientific papers of Ref. [35].

Table 1 Powder XRD experimental findings including lattice cell parameters (*a* and *c*), grain sizes, lattice strain, dislocation density and phase volume fraction parameters of pure and multi-walled carbon nanotube added MgB_2 superconductors

Materials	*a* (Å)	*c* (Å)	Grain size (nm)	Lattice strain (10^{-3})	Ratio of dislocation densities (relative value %)	Phase volume fraction (≈ %)	
						MgB_2	Mg + MgO
0	3.081	3.519	21.503	0.690	–	72	28
1	3.079	3.511	21.369	0.702	9.877	69	31
2	3.077	3.501	20.027	0.704	15.453	66	34
3	3.071	3.498	19.832	0.720	19.410	64	36
4	3.069	3.476	19.684	0.730	24.159	61	39

3.2 Hysteresis curves of pure and multi-walled carbon nanotube added MgB_2 superconductors

In the magnetic characterization parts, the hysteresis (M–H) curves of pure and carbon nanotube added superconductors are examined at 20 K under the external magnetic fields between − 20000 Oe and 20000 Oe. The experimental curves obtained enable us to determine the influence of multi-walled carbon nanotube on the fundamental magnetic quantities such as magnetization values, critical current densities, formation/destruction of flux pinning centers, coupling/decoupling of adjacent layers and beginning point of magnetic field penetration. One can observe the hysteresis curves for all the materials in Fig. 2. It is obvious from the figure that every compound presents the large hysteresis loops (specific to the diamagnetic feature of a material) at 20 K. The main reason with the scenario explained is in association with the fact that the pure and carbon nanotube added MgB_2 superconductors (especially the sample 2) present good and uniform superconductivity.

According to the applied magnetic field strength, the magnetization values are listed as 2, 4, 1, 3 and 0 in descending order. The augmentation in the specific areas (the hysteresis losses) within the M–H curves is anticipated to be the result of the increment in the permanent pinning centers in the crystal lattice. It is appropriate to confirm that the addition of multi-walled carbon nanotubes (serving as the formation of effective nucleation centers along with the trans-granular and intergranular regions) leads to improve significantly the flux pinning strength of MgB_2 material. Besides, it is to be mentioned here that the multi-walled carbon nanotubes act as the artificial defects which can be used for the enhancement in the critical current density [36].

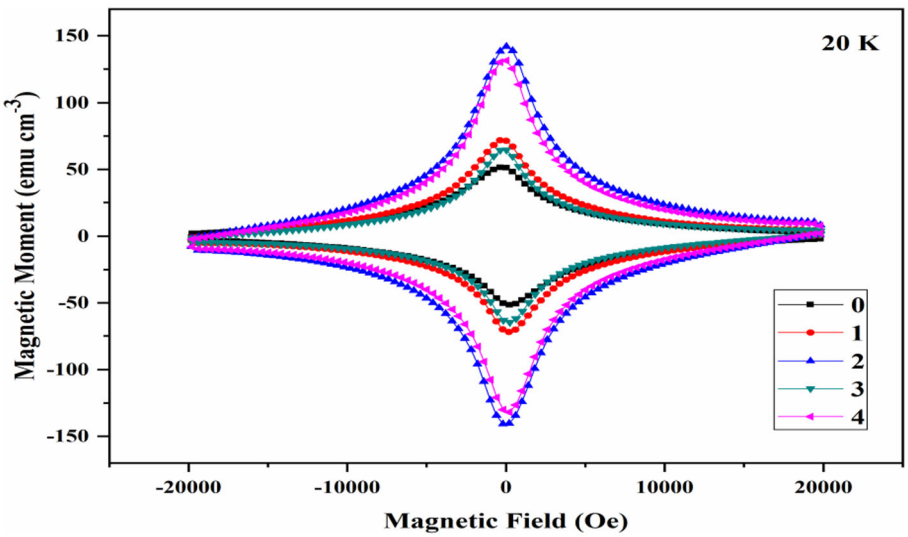

Fig. 2 M–H curves of pure and carbon nanotube added bulk MgB2 superconducting compounds

There seems no break in the M–H curves of samples prepared. Accordingly, the impurity phases present in the structure are not evident. As can be understood from Bean method, the larger hysteresis loops a material has, the higher critical current density the material possesses. In this respect, the sample 2 with the largest hysteresis loops exhibits the highest critical current density values in the magnetic field applied. On the other hand, the pure sample displays the smallest specific area size due to the lack of artificial defects in the crystal lattice. To sum up, the M-H test results verify that the addition of multi-walled carbon nanotubes in the MgB_2 superconducting system plays a positive role on the improvement in the magnetization value and especially flux pinning ability.

3.3 Critical current density calculations founded on Bean model

The hysteresis loops of materials enable us to calculate the critical current densities using Bean model. All the computations are graphically depicted in Fig. 3. It is apparent from the figure that the critical current density parameters inferred are observed to decrease dramatically with the increment in the applied magnetic field strengths. At the zero-field strength, the J_c parameters are obtained to be about 1.0×10^4, 1.3×10^4, 3.2×10^4, 1.4×10^4 and $2.3 \times 10^4 A.cm^{-2}$ for the pure, 1, 2, 3 and 4 materials, respectively. Based on the J_c values, the optimum carbon nanotube addition level is found to be wt. 2% to form artificial pinning centers. Thus, MgB_2 compound exhibits much higher performance on the current carrying at larger magnetic field strengths. Finally, it is necessary to underline that no doubt the addition (causing the artificial defects) presents the positive effect on the critical current density parameters as a result of the increased artificial pinning centers in the crystal lattice, being already confirmed by the areas of hysteresis loops in Fig. 2 and XRD diffraction curves in Fig. 1. The findings are totally favored by the scientific paper in Ref. [21].

3.4 Electrical findings founded on dc resistivity measurements

In this part of paper, we verify the pure and carbon nanotube added bulk MgB_2 compounds driving the superconducting behavior under a critical transition temperature. Thus, we develop a strong link between the fundamental electrical characteristics and addition mechanism in the MgB_2 crystal system. The dc electrical resistivity measurement findings against the temperature range 18–100 K are graphically depicted in Fig. 4. The dc electrical curves allow us to determine the normal state resistivity at room temperature (ρ_{300K}), residual resistivity (ρ_{res}), residual

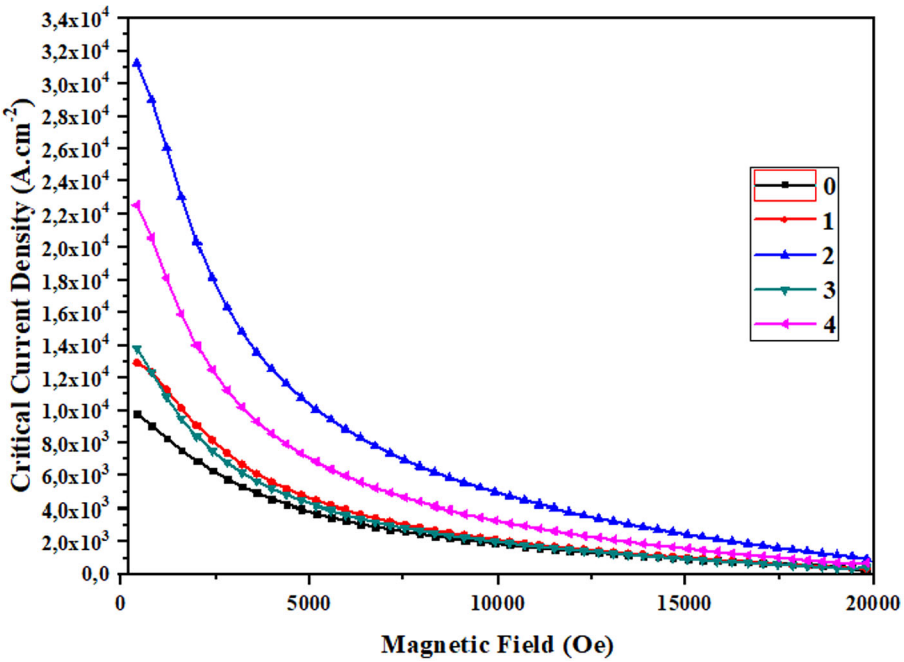

Fig. 3 Variation of critical current densities versus applied magnetic field strengths for samples

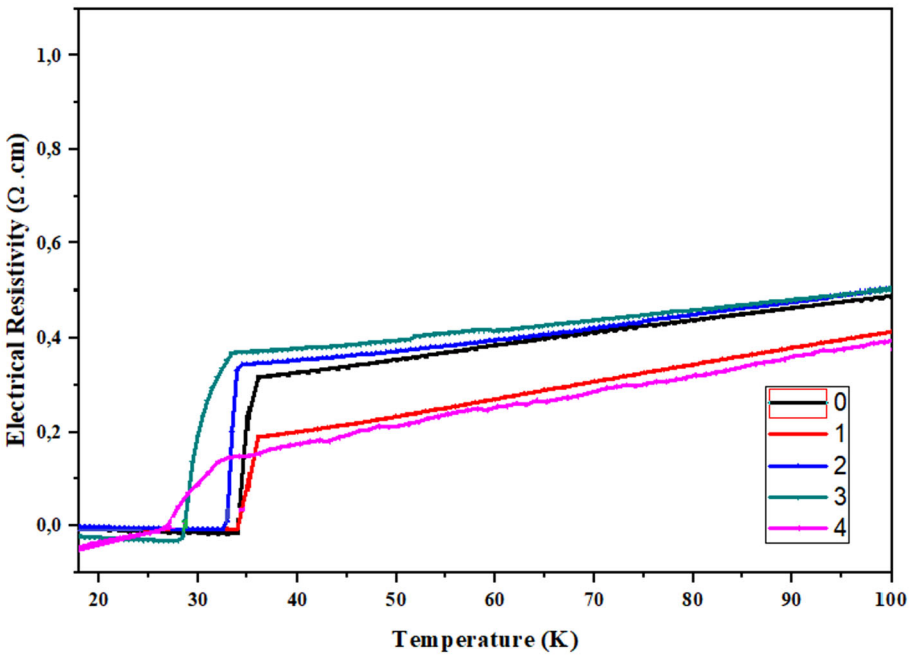

Fig. 4 Temperature-dependent electrical resistivity parameters for every sample prepared in the present work

resistivity ratio (*RRR*), active cross-sectional area fraction (A_F), ρ_{40K}, ρ_{norm}, and $\Delta\rho$ parameters. Figure 4 displays that the fundamental electrical characteristic features are strongly affected by the existence of carbon nanotube. This is attributed to the incorporation of carbon nanotube addition in the MgB_2 crystal matrix. As for the sophisticated interpretations, all the materials studied in the current work show truly metallic transition behavior (metallic character), meaning the linear increment of electrical resistivity with the environment temperature after the onset critical transition temperature values. According to the liquid model approach (interested in the longitudinal transport relaxation rate and separation of spin charge layers), the metallic character results from the logarithmic distribution of active, effective, and dynamic electronic state densities at Fermi energy level [37, 38]. Based on the experimental results, the pure sample shows the highest metallic characteristic nature with fine crystal structure. In other words, the pure sample obtains less local structural defects, porosity, cracks and grain boundary coupling problems in the crystal structure. It is to be stressed here that the addition of carbon nanotube in the crystal system harms the metallic characteristic nature of MgB_2 compound. Similarly, the pure sample exhibits the minimum of normal state resistivity at the room temperature (ρ_{300K}) whereas the other samples produced present rather higher ρ_{300K} values. The increment in the ρ_{300K} parameter is totally related to the enhancement in the permanent structural problems in the crystal structure as well as the degradation in the stabilization of superconducting layers [39].

At the same time, we examine the influence of multi-walled carbon nanotube addition on the evaluated parameters such as ρ_{res}, ρ_{40K}, ρ_{norm}, $\Delta\rho$, *RRR* and A_F. One can see how we are able to determine the values in detail in Ref. [40, 41]. The former parameter (ρ_{res}) to be deduced from Matthiessen's rule [42] directly displays the grain size and metallic connections between the transgranular regions [43]. It is found that the smallest ρ_{res} value of 0.020 mΩcm is observed for the pure sample whereas the increment in the carbon nanotube addition level results in the rapid enhancement towards to the value of 0.630 m Ω cm (Table 2). Thus, the existence of excess multi-walled carbon nanotube in the crystal system damages seriously the crystal structure quality of MgB_2 matrix. Additionally, the second parameter of ρ_{40K} provides about the impurity scattering and lattice strains in the crystal system. According to Table 2, similar to the trend of ρ_{res} parameter the ρ_{40K} parameter for the compounds studied tends to increase systematically with the enhancement in the carbon nanotube addition level. Shortly, the presence of carbon nanotube increases harshly the formation of impurity scattering and lattice strains. In this

Table 2 General electrical resistivity and superconducting measurement results for all the materials studied in the present work

Samples	ρ_{300K} (m Ω cm)	ρ_{res} (m Ω cm)	RRR (ρ_{300K}/ρ_{40K})	ρ_{40K} (m Ω cm)	T_c^{offset} (K)	T_c^{onset} (K)	ΔT_c (K)	A_F
0	1.026	0.020	3.490	0.294	34.0	36.0	2.0	9.988
1	1.041	0.060	3.243	0.321	33.8	35.8	2.0	13.151
2	1.026	0.210	2.889	0.355	32.7	34.3	1.6	10.902
3	1.041	0.380	2.753	0.378	27.9	33.4	5.5	12.031
4	1.074	0.630	2.469	0.435	25.0	32.0	7.0	11.440

respect, the minimum and maximum ρ_{40K} values of 0.294 m Ω cm and 0.435 m Ω cm ascribe to the pure and sample 4, respectively. The third and four terms of $\Delta\rho$ and ρ_{norm} are related to the subtraction of resistivities between ρ_{300K} and ρ_{40K} values, and the ratio of $\rho_{40}/\Delta\rho$, respectively. The parameters are known to be the usage for determining the formation of disorders defects in the crystal system. Shortly, the results about $\Delta\rho$ and ρ_{norm} parameters claim that the increment of carbon nanotube level in the MgB_2 crystal lattice damages gradually the crystal structure quality (founded on the grain size) due to the induced disorders defects in the system. Numerically, the largest $\Delta\rho$ (0.732 m Ω cm) and smallest ρ_{norm} (0.402) values are noted for the pure sample. On the other hand, the sample 4 has the minimum parameter of 6.39 m Ω cm for the $\Delta\rho$ and maximum value of 6.81 for ρ_{norm} parameters, respectively.

We also determine the effect of multi-walled carbon nanotube addition on the residual resistivity ratio ($= \rho_{300k}/\rho_{40k}$, correspondence with the sample production quality) [44] and active cross-sectional area fraction grounded on Rowell's connectivity analysis ($A_F = \rho_{ideal}/[\rho_{300k} - \rho_{40k}]$) [45] where the ρ_{ideal} equals to 7.3 l μΩcm for the bulk MgB_2 superconducting system [46, 47]. It is noteworthy here that the AF parameter illustrates the interaction factor between the coupling superconducting grains in the adjacent layers [45, 46, 48]. The calculated RRR and AF values are depicted in Table 2. According to the table, the former parameter is found to change in a range of 2.469–3.490 whereas the AF parameters are obtained to vary from 9.998 to 11.440. In more detail, the increment in the addition level causes to degrade slightly the parameters. Namely, the greatest RRR value of 3.490 is obtained for the pure sample while the sample 4 possesses the minimum parameter of 2.469 (see in Table 2). It is just the last explanation that the enhancement of multi-walled carbon nanotube level in the bulk MgB_2 superconducting system surpasses slightly the sample quality. To sum up, the pure sample with the larger RRR parameter exhibits the superior crystal quality. At the same time, the RRR results (directly related to the sample quality) display the similar evidence with the AF parameters. The pure sample obtains the smallest AF value of 9.998 whereas the largest value of 13.151 is observed for the sample 2. Rowell analyses present that a material with larger AF parameter has better connection between the coupling superconducting grains in the adjacent layers. On this basis, of the materials studied the sample 2 possesses the greatest interaction between the superconducting grains. Conversely, the sample 1 with the lowest AF value is the worst material among the compounds studied. The dc electrical results indicate that the presence of multi-walled carbon nanotube damages slightly on the general electrical properties of MgB_2 materials due the induced permanent and artificial structural defects, porosity, cracks and grain boundary coupling problems in the crystal system.

3.5 Change of superconducting characteristic properties of MgB_2 with multi-walled carbon nanotube addition

From the dc electrical resistivity measurements, we determine three main transitions: I- offset critical transition temperature (T_c^{offset}), II- onset critical transition (T_c^{onset}) and III- degree of broadening ($\Delta T_c = T_c^{onset} - T_c^{offset}$). The former parameter of T_c^{offset} is a measurement of intergranular component features, and a material exhibits wholly the superconducting phenomenon at such a temperature lower than the T_c^{offset} value due to the presence of coupling formations of cooper-pairs driving the superconductivity [49]. The second one (T_c^{onset}) is connected with the formation of effective and strong electron–

phonon coupling probability in the crystal structure, and is the beginning temperature for the superconductivity. Thus, the isolated grains (intra-granular regions) transit into the superconducting state at the vicinity of T_c^{onset} value [50]. It is obvious that the superconducting nature of a material destroys immediately after the temperature slightly greater than the T_c^{onset} value. The latter parameter of ΔT_c is about the material crystallinity quality. One can see all the parameters for the pure and multi-walled carbon nanotube added MgB_2 superconductors in Table 2. It is visible from the table that both the onset and offset critical transition temperature values tend to decrease regularly (from 36.0 K to 32.0 K and 34.0 K to 25.0 K, respectively) depending on the carbon nanotube addition level in the crystal lattice. In this regard, the pure sample has the highest values of 36.0 K for the T_c^{onset} and 34.0 K for the T_c^{offset} while the sample 4 presents the smallest values of 32.0 K for the T_c^{onset} and 25.0 K for the T_c^{offset} values. It is well known that the critical transition temperature for the MgB_2 material is observed between the values of 34.5 K and 39.4 K [51]. Thus, the experimental finds totally agree with the literature findings. Besides, the decrement in the critical transition temperature values with the addition of SiC, graphite and carbon nanotube is recorded in Ref. [35]. However, interestingly the pure sample indicates the middle value of 2.0 K for the ΔT_c parameter whereas the smallest ΔT_c value is obtained to be about 1.6 K for the sample 2. On the other hand, the largest one (7.0 K) belongs to the sample 4. This fact has already been confirmed by the XRD and M-H measurement tests. At the same time, it would be more precise to claim that the addition level causes to change only the value of two-gap energy states instead of the destruction of them.

To sum up, even though the carbon nanotube addition in the MgB_2 crystal structure is ploughed to enhance the general electrical features, grain size, onset and offset critical transition temperatures, the other crucial properties (crystallinity, degree of broadening, magnetization values, coupling of adjacent layers and flux pinning ability) for the application fields in the heavy-industrial technology and energy-related sectors are found to improve remarkably in case of the optimum dopant level. The experimental results deduced are found to show a good agreement with previous studies in the literature [52–55]. Besides, it has been reported that the contribution of many different carbon sources, carbon nanotubes and related materials has a positive effect on the critical current density and magnetization values in the bulk MgB_2 superconducting material while reducing the critical transition temperatures [21, 52–55].

All the findings in the paper enable us to discuss electrodynamically the change in the clean/dirty limit characteristic nature of MgB_2 superconducting compound with the carbon nanotube addition in the crystal system with the aid of grounded theory approach. It is well known that the fundamental aspects of electrodynamic are related to two main parameters: electronic mean free path (l) and coherence length (ξ). In case the former parameter of l is larger than the coherence length, the material studied is within the clean limit [56, 57]. The MgB_2 superconducting compound is received to exhibit the clean limit feature. Further, it was reported in 1959 that the dirty samples carry rather larger current when the high magnetic field is applied [58]. Hence, these kinds of materials are indispensable candidate for the practical applications. However, the dirty materials are insensitive to any foreign intervention. Accordingly, the production of dirty compound from the clean material (with the change of material preparation procedures) has attracted remarkable interest in the recent years. In this respect, the multi-walled carbon nanotube addition (especially weight ratio of 2%) in the crystal system makes the MgB_2 compound bring closer to the dirty limit.

3.6 Variation in gap coefficients for electron–phonon couplings of carbon nanotube added MgB_2 materials

In the present study, the influence of carbon nanotube on the scattering or breaking mechanism (related to the pair binding energy) of super-electrons is explored depending on the variation of gap coefficient parameters at any temperature values lower than critical transition temperature. As well known that the order parameter introduced by Bardeen, Cooper and Schrieffer is related to the gap coefficient (energy gap, Δ) quantity, and the numerical value of parameter is used to define the type (type-I or type-II) of superconducting material. The higher value a material possesses the greater critical transition temperature the compound exhibits. At the same time,

the gap coefficient enables us to determine the formation mechanism of excited electrons in conduction bands or electron–phonon couplings (super-electrons) in the superconducting crystal matrix. Besides, the Δ value is responsible for the variation of main thermodynamics quantities (enthalpy, latent heat, entropy, specific heat, Gibbs and Helmholtz free energy) of a compound. As a result of the scientific research performed so far, the temperature-dependent gap coefficient ($2\Delta/k_BT_c$ at around 0 K) parameters were found to be about 3.52 for the type-I superconducting system with the BCS weak-coupling in the basal plane and 6.2 for the type-II superconducting system with strongly coupled systems [59–61]. It is obvious that the superconducting material with higher energy coefficient shows greater electron pair binding energy. In this regard, the energy interval (2Δ) parameter is the minimum energy required for breaking up the pair binding energy. At any finite temperature values lower than critical transition temperature ($T \neq 0$ K) the superconducting compound obtains both the electron–phonon couplings (super-electrons) and single electrons (density of excitations) in the crystal system. It has already known that the number related to the excited electrons or super-electrons in the system is significantly affected by the operating (ambient) temperature. Depending on the temperature, both the collision for the excited electrons in conduction bands and scattering mechanisms (with low energic phonons) of cooper-pairs play dominant role in the superconducting system due to larger energy value than energy interval value. Hence, the number of normal electrons (super-electrons) increases (decreases) considerably in the superconducting matrix. Once the operating temperature equals the critical transition temperature, the gap coefficient disappears immediately, and the superconductivity phenomenon destroys. However, it is to be mentioned here that at relatively lower temperatures the cooper-pairs are alive for the superconductivity and hardly any scattered in the superconducting crystal lattice due to the insufficient energy of electrons to be able to excite to the higher states. In addition to the operating temperature, the preparation conditions cause to vary the gap coefficient values of superconducting materials.

There are two different energy gap parameters (related to the σ-band and π-band) in the superconducting MgB_2 material. The half-widths Δ(T = 0) of two gaps are experimentally measured to be in a range of 6.5–8.0 meV and 1.9–2.8 meV for the $\Delta\sigma(0)$ and $\Delta\pi(0)$ energy, respectively [62–66]. Obviously, the former value is recorded to be slightly larger in comparison with the value of Δ(0) = 3.52 found for the BCS weak-coupling in the type-I superconducting system whereas the latter one is a little lower than the value of 3.52. Although there appear considerable different energy scales for the two gaps in the superconducting MgB_2 compound, the gap coefficients approach each other at the same temperature due to the coupling between the σ- and π-bands. Accordingly, the MgB_2 system possesses a single transition temperature such a temperature of 39 K [67]. Moreover, the temperature-dependent half-width of energy gap Δ(0) was theoretically examined by Choi et al. [68] and by Brinkman et al. [69]. According to the approximation performed by Choi et al. [68], the fitting gap energy parameters were taken as Δ(0) = 6.8 meV for the σ gap and Δ(0) = 1.8 meV for the π gap. The related exponential values of p were found to be 2.9 and 1.8 for the σ gap and π gap coefficients, respectively. In the current work, we determine the effect of carbon nanotube addition on the two energy gap parameters using the approximation depending on the Δ(0) and p values by means of following equations [69–71]:

$$\frac{2\Delta_\sigma(0)}{K_BT_c} = 4.05 \, and \, \frac{2\Delta_\pi(0)}{K_BT_c} = 1.07 \quad (6)$$

[53, 59]

$$\Delta(T) = \Delta(0)\left[1 - \left(\frac{T}{T_c}\right)p\right]^{1/2} \quad (7)$$

In Eq. 5, the equalities of 4.05 and 1.07 are determined with respect to 6.8 meV and 1.8 meV of $\Delta_{\sigma 0}$ and $\Delta_{\pi 0}$ gap energy values. In Eq. 6, according to Choi approximation the exponential values of p are taken to be 2.9 and 1.8 for the σ gap and π gap coefficients for defining the $\Delta_\sigma(T)$ and $\Delta_\pi(T)$. With the use of scientific relations, the energy gap parameters are calculated at the various temperatures lower than the transition temperatures of carbon nanotube added MgB_2 superconducting materials.

All the obtained curves with the weak and strong-coupling characteristics of superconducting state in the basal plane are depicted in Fig. 5i, ii. It is apparent from Fig. 5 that the gap coefficients are observed to diminish dramatically as the carbon nanotube

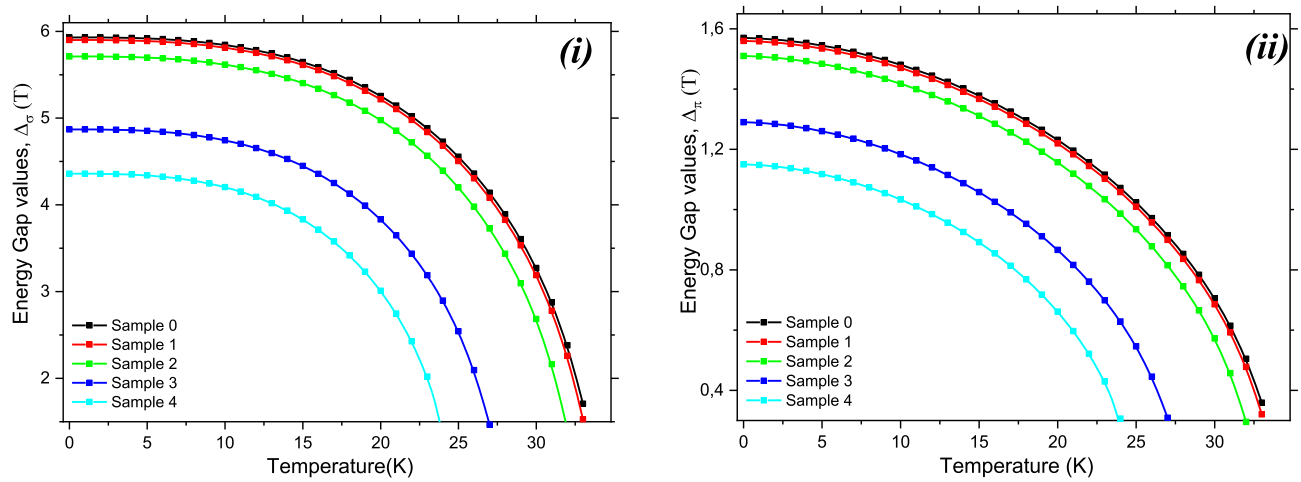

Fig. 5 Differentiations of energy gaps of **i** σ-bands and **ii** π-bands against operating temperature for all MgB_2 materials prepared

addition level increases in the crystal system. The decrement confirms that the presence of excess carbon nanotube in the system degrades the minimum energy required for breaking up the pair binding energy. Accordingly, the scattering/breaking of cooper-pairs in the small homogeneous clusters in the superconducting paths of bulk MgB_2 system enhances considerably depending on the increase of normal electrons in the conduction bands. Numerically, the $\Delta_{\sigma 0}$ ($\Delta_{\pi 0}$) gap energy values are determined to be about 5.93 (1.57) eV, 5.90 (1.56) eV, 5.71 (1.51) eV, 4.87 (1.29) eV and 4.36 (1.15) eV for the pure, 1, 2, 3 and 4 sample, respectively.

4 Conclusion

In the present work, the influence of carbon nanotube addition levels within the different molecular weight ratios of 0–4% on some fundamental electrical, superconducting and magnetic features of bulk MgB_2 material is examined by means of the standard temperature-dependent electrical resistivity, powder X-ray diffraction, and magnetization measurements. It is noted that even though the presence of carbon nanotube in the crystal system damages slightly the crystallinity and superconducting transition temperatures, the carbon nanotube added MgB_2 compounds begin to show relatively higher magnetization values, flux pinning strength and critical current densities at the applied magnetic fields. The latter parameters for the superconductor materials extremely play the vital roles on the application areas in the heavy-industrial technology and energy-related sectors. In more detail, the optimum addition (2%) mechanism leads to improve remarkably the effective nucleation centers (behaving as the artificial pinning centers) throughout the intra-granular and intergranular regions in the crystal system, magnetization value and especially flux pinning strength of MgB_2 material. Additionally, the gap coefficient investigations show that the excess carbon nanotube addition in the MgB_2 system truncates the minimum energy required for breaking up the pair binding energy. All in all, the addition of carbon nanotube may be a good preference for the MgB_2 superconducting materials to find more application areas.

Acknowledgements

We would like to express our gratitude to the Kastamonu University Central Research Laboratory and Gazi University Thermal Analysis Laboratory who contributed to this study.

References

1. J. Nagamatsu, N. Nakagawa, T. Muranaka, Y. Zenitani, J. Akimitsu, Superconductivity at 39 K in magnesium diboride. Nature **410**(6824), 63–64 (2001). https://doi.org/10.1038/35065039
2. D. Rodrigues Jr., L.H.M. Antunes, A.L.R. Manesco, E.M. Moraes, L.B.S. da Silva, Development and characterization of Cu–Nb–MgB_2 and CuNi–Nb–MgB_2 Wires with VB_2 and

carbon nanotube additions. IEEE Trans. Appl. Supercon. **25**, 3 (2015)
3. E.W. Collings, E. Lee, M.D. Sumption, M. Tomsic, X.L. Wang, S. Soltanian, S.X. Dou, Continuous- and batch-processed MgB_2/Fe strands-transport and magnetic properties. Physica C **386**, 555–559 (2003). https://doi.org/10.1016/S0921-4534(02)02174-3
4. T. Matsushita, M. Kiuchi, E.S. Otabe, A. Yamamoto, J. Shimoyama, K, Kishio, Critical current properties at high magnetic fields in polycrystalline MgB_2 superconductors. Physica C. **470**(20), 1406–1410 (2010). https://doi.org/10.1016/j.physc.2010.05.124
5. M.A. Aksan, M.E. Yakıncı, A. Güldeste, Co-addition into MgB_2: the structural and electronic properties of $(MgB_2)_{2-x}Co_x$. J. Alloy. Compd. **424**(1–2), 33–40 (2006). https://doi.org/10.1016/j.jallcom.2005.12.066
6. B. Qu, X.D. Sun, J.-G. Li, Z.M. Xiu, S.H. Liu, C.P. Xue, Significant improvement of critical current density in MgB_2 doped with ferromagnetic Fe_3O_4 nanoparticles. Supercond. Sci. Technol. **22**(1), 015027 (2008). https://doi.org/10.1088/0953-2048/22/1/015027
7. A. Berenov, A. Serquis, X.Z. Liao, Y.T. Zhu, D.E. Peterson, Y. Bugoslavsky, K.A. Yates, M.G. Blamire, L.F. Cohen, J.L. MacManus-Driscoll, Enhancement of critical current density in low level Al-doped MgB_2. Supercond. Sci. Technol. (2004). https://doi.org/10.1088/0953-2048/17/10/001
8. S. Ueda, J. Shimoyama, A. Yamamoto, S. Horii, K. Kishio, Enhanced critical current properties observed in Na_2CO_3-doped MgB_2. Supercond. Sci. Technol. **17**(7), 926–930 (2004). https://doi.org/10.1088/0953-2048/17/7/017
9. X. Zhang, D. Wang, Z. Gao, L. Wang, Y. Ma, Z. Qi, K. Watanabe, The doping effect of activated carbon on the superconducting properties of MgB_2 tapes. Supercond. Sci. Technol. **21**, 075008 (2008)
10. L.B.S. Da Silva, D. Rodrigues Jr., G. Serrano, V.C.V. Metzner, M.T. Malachevsky, A. Serquis, MgB_2 superconductors with addition of other diborides and SiC. IEEE Trans. Appl. Supercond. **21**, 2639–2642 (2011)
11. T. Masui, S. Lee, S. Tajima, Carbon-substitution effect on the electronic properties of MgB_2 single crystals. Phys. Rev. B **70**, 024504 (2004)
12. R.H.T. Wilke, S.L. Bud'ko, P.C. Canfield, D.K. Finnemore, R.J. Suplinskas, S.T. Hannahs, Systematic effects of carbon doping on the superconducting properties of $Mg(B_{1-x}C_x)_{(2)}$. Phys. Rev. Lett. **92**, 217003 (2004)
13. L. Chunyan, S. Hongli, L. Min, M. Lin, W. Yi, T. Min, W. Baicen, C. Jin, J. Yaotang, Effect of malonic acid and of different doping methods on the superconducting properties of MgB2 superconductors. Physica C **555**, 60–65 (2018). https://doi.org/10.1016/j.physc.2018.10.011
14. W.K. Yeoh, J. Horvat, S.X. Dou, P. Munroe, Effect of carbon nanotube size on superconductivity properties of MgB_2. IEEE Trans. Appl. Supercond. **15**(2), 3284–3287 (2005). https://doi.org/10.1109/TASC.2005.848853
15. C.H. Cheng, H. Zhang, Y. Zhao, Y. Feng, X.F. Rui, P. Munroe, H.M. Zeng, N. Koshizuka, M. Murakami, Doping effect of nano-diamond on superconductivity and flux pinning in MgB_2. Supercond. Sci. Technol. **16**(10), 1182–1186 (2003). https://doi.org/10.1088/0953-2048/16/10/310
16. S. Soltanian, J. Horvat, X.L. Wang, P. Munroe, S.X. Dou, Effect of nano-carbon particle doping on the flux pinning properties of MgB_2 superconductor. Physica C **390**(3), 185–190 (2003). https://doi.org/10.1016/S0921-4534(03)00960-2
17. S.J. Ye, A. Matsumoto, Y.C. Zhang, H. Kumakura, Strong enhancement of high-field critical current properties and irreversibility field of MgB_2 superconducting wires by coronene active carbon source addition via the new B powder carbon-coating method. Supercond. Sci. Technol. **27**(8), 085012 (2014). https://doi.org/10.1088/0953-2048/27/8/085012
18. S. Iijima, Helical microtubules of graphitic carbon. Nature **354**, 56–58 (1991). https://doi.org/10.1038/354056a0
19. D. Patel, M. Maeda, S. Choi, S.J. Kim, M. Shahabuddin, M.P. Japar, S. Hossain, J.H. Kim, Multiwalled carbon nanotube-derived superior electrical, mechanical and thermal properties in MgB_2 wires. Scripta Mater. **88**, 13–16 (2014). https://doi.org/10.1016/j.scriptamat.2014.06.010
20. J.H. Kim, W.K. Yeoh, X. Xu, S.X. Dou, P. Munroe, M. Rindfleisch, M. Tomsic, Superconductivity of MgB_2 with embedded multiwall carbon nanotube. Physica C **449**(2), 133–138 (2006). https://doi.org/10.1016/j.physc.2006.08.003
21. S.X. Dou, W.K. Yeoh, J. Horvat, M. Ionescu, Effect of carbon nanotube doping on critical current density of MgB_2 superconductor. Appl. Phys. Lett. **83**, 4996 (2003). https://doi.org/10.1063/1.1634378
22. C. Shekhar, R. Giri, S.K. Malik, O.N. Srivastava, Improved critical current density of MgB_2—carbon nanotubes (CNTs) composite. J. Nanosci. Nanotechnol. **7**(6), 1804–1809 (2007). https://doi.org/10.1166/jnn.2007.720
23. W.K. Yeoh, J.H. Kim, J. Horvat, S.X. Dou, P. Munroe, Improving flux pinning of MgB_2 by carbon nanotube doping and ultrasonication. Supercond. Sci. Technol. **19**, L5–L8 (2006). https://doi.org/10.1088/0953-2048/19/2/L01
24. P. Kováč, I. Hušek, V. Skákalova, J. Meyer, E. Dobročka, M. Hirscher, S. Roth, Transport current improvements of in situ MgB_2 tapes by the addition of carbon nanotubes, silicon carbide or graphite. Supercond. Sci. Technol. **20**(1), 105–111 (2007). https://doi.org/10.1088/0953-2048/20/1/019

25. W.X. Li, Y. Li, R.H. Chen, W.K. Yoeh, S.X. Dou, Effect of magnetic field processing on the microstructure of carbon nanotubes doped MgB_2. Physica C. **460–462**(1), 570–571 (2007). https://doi.org/10.1016/j.physc.2007.04.139
26 A. Serquis, G.P. Serrano, S.M. Moreno, L. Civale, B. Maiorov, F. Balakirev, M. Jaime, Correlated enhancement of Hc2 and Jc in carbon nanotube doped MgB_2. Supercond. Sci. Technol. **20**(4), L12–L15 (2007). https://doi.org/10.1088/0953-2048/20/4/L02
27. Q. Cai, Y. Liu, Z. Ma, D.A. Cardwell, Fishtail effects and improved critical current density in polycrystalline bulk MgB_2 containing carbon nanotubes. Physica C **492**, 6–10 (2013). https://doi.org/10.1016/j.physc.2013.05.002
28. S.X. Dou, W.K. Yeoh, O. Shcherbakova, D. Wexler, Y. Li, Z.M. Ren, P. Munroe, S.K. Chen, K.S. Tan, B.A. Glowacki, J.L. MacManus-Driscoll, Alignment of carbon nanotube additives for ımproved performance of magnesium diboride superconductors. Adv. Mater. **18**(6), 785–788 (2006). https://doi.org/10.1002/adma.200501617
29. C. Suryanarayana, M.G. Norton, *X-Ray diffraction a practical approach*, vol. 212 (Plenum Publishing Corporation, New York, 1998), pp. 3–19
30. C.P. Bean, Magnetization of hard superconductors. Phys. Rev. Lett. **8**, 250–253 (1962). https://doi.org/10.1103/PhysRevLett.8.250
31. Z.K. Liu, Y. Zhong, D.G. Schlom, X.X. Xi, Q. Li, Computational thermodynamic modeling of the Mg–B system. Calphad **25**, 299–303 (2001)
32. P.M. Shafi, A.C. Bose, Impact of crystalline defects and size on X-ray line broadening: a phenomenological approach for tetragonal SnO_2 nanocrystals. AIP Adv. **5**, 057137 (2015). https://doi.org/10.1063/1.4921452
33. W.Z. Zhu, D.E. Miser, W.G. Chan, M.R. Hajaligol, Characterization of multiwalled carbon nanotubes prepared by carbon arc cathode deposit. Mater. Chem. Phys. **82**(3), 638–647 (2003). https://doi.org/10.1016/S0254-0584(03)00341-9
34. J.H. Kim, W.K. Yeoh, M.J. Qin, X. Xu, S.X. Dou, The doping effect of multiwall carbon nanotube on MgB_2/Fe superconductor wire. J. Appl. Phys. **100**(1), 013908 (2006). https://doi.org/10.1063/1.2209188
35 L.B.S. Da Silva, E.E. Hellstrom, D. Rodrigues Jr., MgB_2 superconductors with addition of ZrB2 and different carbon sources. J. Phys. **507**, 012043 (2014)
36. W.K. Yeoh, J. Horvat, S.X. Dou, V. Keast, Strong pinning and high critical current density in carbon nanotube doped MgB_2. Supercond. Sci. Technol. **17**(9), 572–577 (2004). https://doi.org/10.1088/0953-2048/17/9/022
37. P.B. Allen, W.E. Pickett, H. Krakauer, Anisotropic normal-state transport-properties predicted and analyzed for high-Tc oxide superconductors. Phys. Rev. B **37**(13), 7482–7490 (1988). https://doi.org/10.1103/PhysRevB.37.7482
38. P.W. Anderson, Hall effect in the two-dimensional luttinger liquid. Phys. Rev. Lett. **67**, 2092 (1991). https://doi.org/10.1103/PhysRevLett.67.2092
39. Y. Zalaoglu, G. Yildirim, H. Büyükuslu, N.K. Saritekin, A. Varilci, C. Terzioglu, O. Gorur, Important defeats on pinning of 2D pancake vortices in highly anisotropic Bi-2212 superconducting matrix with homovalent Bi/La substitution. J. Alloys Compd. (2015). https://doi.org/10.1016/j.jallcom.2015.01.095
40. S.B. Guner, Y. Zalaoglu, T. Turgay, O. Ozyurt, A.T. Ulgen, M. Dogruer, G. Yildirim, A detailed research for determination of Bi/Ga partial substitution effect in Bi-2212 superconducting matrix on crucial characteristic features. J. Alloy. Compd. **772**, 388–398 (2019). https://doi.org/10.1016/j.jallcom.2018.09.071
41. A.T. Ulgen, T. Turgay, C. Terzioglu, G. Yildirim, M. Oz, Role of Bi/Tm substitution in Bi-2212 system on crystal structure quality, pair wave function and polaronic states. J. Alloys Compd. **764**, 755–766 (2018). https://doi.org/10.1016/j.jallcom.2018.06.142
42 J. Ekin, *Experimental techniques for low-temperature measurements: cryostat design, material properties and superconductor critical-current testing* (Oxford University Press, New York, 2006)
43. B.D. Cullity, S.R. Stock, *Elements of x-ray diffraction*, 3rd edn. (Pearson, USA, 2014)
44. X. Xu, J.H. Kim, S.X. Dou, S. Choi, J.H. Lee, H.W. Park, M. Rindeish, M. Tomsic, A correlation between transport current density and grain connectivity in MgB_2/Fe wire made from ball-milled boron. J. Appl. Phys. **105**, 103913 (2009). https://doi.org/10.1063/1.3129314
45. J.M. Rowell, The widely variable resistivity of MgB_2 samples. Supercond. Sci. Technol. **16**(6), R17 (2003). https://doi.org/10.1088/0953-2048/16/6/201
46. J. Jiang, B.J. Senkowicz, D.C. Larbalestier, E.E. Hellstrom, Influence of boron powder purification on the connectivity of bulk MgB_2. Supercond. Sci. Technol. **19**(8), L33 (2006). https://doi.org/10.1088/0953-2048/19/8/L02
47. R.H.T. Wilke, S.L. Bud'ko, P.C. Canfield, D.K. Finnemore, R.J. Suplinskas, S.T. Hannahs, Synthesis and optimization of $Mg(B_{1-x}C_x)_2$ wire segments. Physica C. **424**, 1–16 (2005). https://doi.org/10.1016/j.physc.2005.04.016
48. M. Dogruer, G. Yildirim, C. Terzioglu, Effect of diffusion-annealing time on magnetoresistivity of Cu-diffused bulk MgB_2 superconductors with experimental and theoretical approaches. J. Mater. Sci. **24**, 958–967 (2012). https://doi.org/10.1007/s10854-012-0857-8

49 R. Awad, A.I. Abou-Aly, M.M.H. Abdel Gawad, I. G-Eldeen, The influence of SnO_2 nano-particles addition on the vickers microhardness of (Bi, Pb)-2223 superconducting phase. J. Superconduct. Novel Magnet. **25**, 739–745 (2012). https://doi.org/10.1007/s10948-011-1334-y

50. A. Ianculescu, M. Gartner, B. Despax, V. Bley, Th. Lebey, R. Gavrila, M. Modreanu, Optical characterization and microstructure of BaTiO(3) thin films obtained by RF-magnetron sputtering. Appl. Surf. Sci. **253**(1), 344–348 (2006). https://doi.org/10.1016/j.apsusc.2006.06.008

51. T.A. Prikhna, Properties of MgB_2 bulk, Institute for superhard materials of the national academy of sciences of Ukraine, Arxiv ResearchGate. (2014)

52. S.X. Dou, S. Soltanian, X.L. Wang, P. Munroe, S.H. Zhou, M. Ionescu, H.K. Liu, M. Tomic, Enhancement of the critical current density and flux pinning of MgB_2 superconductor by nanoparticle SiC doping. Appl. Phys. Lett. **81**(18), 3419–3421 (2002). https://doi.org/10.1063/1.1517398

53 R.A. Ribeiro, S.L. Bud'ko, C. Petrovic, P.C. Canfield, Carbon doping of superconducting magnesium diboride. Physica C **384**(3), 227–236 (2003). https://doi.org/10.1016/S0921-4534(02)02331-6

54. A. Yamamoto, J. Shimoyama, S. Ueda, I. Iwayama, S. Horii, K. Kishio, Effects of B_4C doping on critical current properties of MgB_2 superconductor. Supercond. Sci. Technol. **18**(10), 1323 (2005). https://doi.org/10.1088/0953-2048/18/10/012

55. T. Dilek, E.T. Koparan, M. Başoğlu, E. Yanmaz, The magnetic and structural properties of SiC-doped MgB_2 bulks prepared by the standard ceramic processing. J. Superconduct. Novel Magnet **24**(1), 495–497 (2011). https://doi.org/10.1007/s10948-010-0979-2

56. M. Dressel, G. Guner, *Electrodynamics of solids, optical properties of electrons in matter*, 1st edn. (University Press, Cambridge, 2002)

57. B.B. Jin, T. Dahm, C. Iniotakis, A.I. Gubin, E.M. Choi, H.J. Kim, S.-I.K. Lee, W.N. Kang, S.F. Wang, Y.L. Zhou, A.V. Pogrebnyakov, J.M. Redwing, X.X. Xi, N. Klein, Dependence of penetration depth, microwave surface resistance and energy gap of MgB2 thin films on their normal-state resistivity. Supercond. Sci. Technol. **18**, L1 (2005). https://doi.org/10.1088/0953-2048/18/1/L01

58 P.W. Anderson, Theory of dirty superconductors. J. Phys. Chem. Solids **11**(1–2), 26–30 (1959). https://doi.org/10.1016/0022-3697(59)90036-8

59 N. Hudakova, P. Samuely, P. Szabo, V. Plecháček, K. Knížek, D. Sedmidubskyý, Scaling of the superconducting order parameter in Bi cuprates with Tc. Physica C. **246**, 163–168 (1995). https://doi.org/10.1016/0921-4534(95)00160-3

60 A.V. Narlikar, *Superconductors*, 1st edn. (Oxford Press, Oxford, 2014)

61 R. Wesche, *Physical properties of high-temperature superconductors*, 1 Kindle. (Wiley, Chichester, 2015)

62. M.R. Eskildsen, M. Kugler, G. Levy, S. Tanaka, J. Jun, S.M. Kazakov, J. Karpinski, O. Fischer, Scanning tunneling spectroscopy on single crystal MgB_2. Physica C. **385**, 169–176 (2003). https://doi.org/10.1016/S0921-4534(02)02301-8

63. R.S. Gonnelli, D. Daghero, G.A. Ummarino, V.A. Stepanov, J. Jun, S.M. Kazakov, J. Karpinski, Direct evidence for two-band superconductivity in MgB_2 single crystals from directional point-contact spectroscopy in magnetic fields. Phys. Rev. Lett. **89**, 247004 (2002). https://doi.org/10.1103/PhysRevLett.89.247004

64. Z.Z. Li, H.J. Tao, Y. Xuan, Z.A. Ren, G.C. Che, B.-R. Zhao, Andreev reflection spectroscopy evidence for multiple gaps in MgB_2. Phys. Rev. B **66**, 064513 (2002). https://doi.org/10.1103/PhysRevB.66.064513

65. S. Lee, Z.G. Khim, Y. Chong, S.H. Moon, H.N. Lee, H.G. Kim, B. Oh, E.J. Choi, Measurement of the superconducting gap of MgB_2 by point contact spectroscopy. Physica C. **377**, 202–207 (2002). https://doi.org/10.1016/S0921-4534(02)01349-7

66. P. Szabo, P. Samuely, J. Kačmarčík, T. Klein, J. Marcus, D. Fruchart, S. Miraglia, C. Marcenat, A.G.M. Jansen, Evidence for two superconducting gaps in MgB_2 by point-contact spectroscopy. Phys. Rev. Lett. **87**, 137005 (2001). https://doi.org/10.1103/PhysRevLett.87.137005

67. D. Daghero, R.S. Gonnelli, Probing multiband superconductivity by point-contact spectroscopy. Supercond. Sci. Technol. **23**, 043001 (2010). https://doi.org/10.1088/0953-2048/23/4/043001

68. H.J. Choi, M.L. Cohen, S.G. Louie, Anisotropic Eliashberg theory of MgB_2: T_c, isotope effects, superconducting energy gaps, quasiparticles, and specific heat. Physica C. **385**, 66–74 (2003). https://doi.org/10.1016/S0921-4534(02)02345-6

69. A. Brinkman, A.A. Golubov, H. Rogalla, O.V. Dolgov, J. Kortus, Y. Kong, O. Jepsen, O.K. Andersen, Multiband model for tunneling inMgB_2 junctions. Phys. Rev. B. **65**, 180517(R) (2002). https://doi.org/10.1103/PhysRevB.65.180517

70. M. Cyrot, D. Pavuna, *Introduction to superconductivity and high-Tc materials*, 1st edn. (World Scientific Publishing Company, Singapore, 1992)

71. A.K. Saxena, *High-temperature superconductors*, 2nd edn. (Springer, New York, 2012)